Cellular Microbiology (2014) **16**(5), 642–656
doi:10.1111/cmi.12287
First published online 27 March 2014

Conditional expression of apical membrane antigen 1 in *Plasmodium falciparum* shows it is required for erythrocyte invasion by merozoites

Alan Yap,[1] Mauro F. Azevedo,[2] Paul R. Gilson,[2] Greta E. Weiss,[2] Matthew T. O'Neill,[1] Danny W. Wilson,[1] Brendan S. Crabb[2] and Alan F. Cowman[1]*

[1]*The Walter and Eliza Hall Institute of Medical Research, Melbourne, Vic. 3052, Australia.*
[2]*Macfarlane Burnet Institute for Medical Research & Public Health, Melbourne, Vic. 3004, Australia.*

Summary

Malaria is caused by obligate intracellular parasites, of which *Plasmodium falciparum* is the most lethal species. In humans, *P. falciparum* merozoites (invasive forms of the parasite) employ a host of parasite proteins to rapidly invade erythrocytes. One of these is the *P. falciparum* apical membrane antigen 1 (PfAMA1) which forms a complex with rhoptry neck proteins at the tight junction. Here, we have placed the *Pfama1* gene under conditional control using dimerizable Cre recombinase (DiCre) in *P. falciparum*. DiCre-mediated excision of the loxP-flanked *Pfama1* gene results in approximately 80% decreased expression of the protein within one intraerythrocytic growth cycle. This reduces growth by 40%, due to decreased invasion efficiency characterized by a post-invasion defect in sealing of the parasitophorous vacuole. These results show that PfAMA1 is an essential protein for merozoite invasion in *P. falciparum* and either directly or indirectly plays a role in resealing of the red blood cell at the posterior end of the invasion event.

Introduction

Malaria, which is caused by *Plasmodium* parasites, remains a major public health problem in large parts of sub-Saharan Africa, tropical and subtropical regions of Asia and the Americas. *Plasmodium falciparum* is the most lethal species that infect humans (Snow *et al*., 2005), although *Plasmodium vivax* is gaining importance as a major cause of malaria mortality and morbidity outside Africa (Guerra *et al*., 2010). *Plasmodium* parasites passage between the mosquito vector and human host to complete their multi-stage development, adopting multiple invasive 'zoite' forms throughout the process. In humans, sporozoites are injected into the skin by female *Anopheles* mosquitoes infected with malaria and they rapidly invade hepatocytes to initiate the liver stage infection. These intracellular parasites develop into exoerythrocytic merozoites that are released into the bloodstream where they invade circulating erythrocytes. As obligate intracellular parasites, merozoites mature within erythrocytes and develop cyclically through ring, trophozoite and schizont stages inside a compartment termed the parasitophorous vacuole. At the final stage of development, the parasite undergoes asexual division (schizogony) to produce 16–32 daughter merozoites that are released upon egress to invade new erythrocytes.

Invasion of erythrocytes by merozoites is a complex and multistep process (reviewed in Cowman and Crabb, 2006). At egress an infected erythrocyte bursts releasing merozoites that can attach to uninfected erythrocytes. The low potassium level in the bloodstream triggers intracellular calcium release activating sequential release of micronemes and rhoptries, which are apical secretory organelles that secrete proteins involved in the invasion process (Singh *et al*., 2010). Once attached to an erythrocyte, the merozoite reorientates its apical end to the erythrocyte surface and an interface forms between the two cells; a tight junction composed of parasite proteins around the periphery of the merozoite apex on the cross-sectional plane of invasion. Active invasion ensues as the merozoite slides through the tight junction, which moves from anterior to posterior end of the parasite cell. As the merozoite penetrates the erythrocyte, proteins and lipids are released from apical organelles into a pocket formed primarily from the invaginating erythrocyte membrane (Suss-Toby *et al*., 1996; Gruring *et al*., 2011; Riglar *et al*., 2011). After the merozoite has completely entered the erythrocyte, the membrane is closed forming the parasitophorous vacuole and re-sealing the erythrocyte membrane. As this takes place, the erythrocyte

Received 23 December, 2013; revised 23 February, 2014; accepted 24 February, 2014. *For correspondence. E-mail cowman@wehi.edu.au; Tel. (+61) 393 452 555; Fax (+61) 393 470 852.

undergoes 5–10 min of echinocytosis (transient spike-like extrusions of the erythrocyte membrane possibly caused by dehydration) before the infected erythrocyte reverts to its normal shape (Gilson and Crabb, 2009). By this time, the merozoite has differentiated into an amoeboid ring-stage parasite (Gruring *et al*., 2011; Riglar *et al*., 2011).

Apical membrane antigen 1 is one of a number of proteins released from the parasite micronemes, and it is a type I integral membrane protein synthesized in segmenting schizonts as an 83 kDa precursor protein. When AMA1 is secreted onto the merozoite surface prior to schizont rupture the prodomain is cleaved leaving a 66 kDa membrane-bound species (Crewther *et al*., 1990; Narum and Thomas, 1994; Howell *et al*., 2001). AMA1 homologues exist in most apicomplexan parasites including all *Plasmodium* species sequenced to date, *Toxoplasma gondii* and *Babesia divergens* (Donahue *et al*., 2000; Montero *et al*., 2009). The ectodomains of AMA1 in *Plasmodium* share a similar tertiary structure suggesting a conserved role (Bai *et al*., 2005). Paradoxically, AMA1 is also a highly polymorphic protein with variation of approximately 10% of the amino acids (Chesne-Seck *et al*., 2005). These sequence polymorphisms contribute to antibody escape and are therefore a major hurdle to generating an effective AMA1 vaccine (Healer *et al*., 2004). Nonetheless, AMA1 is a leading blood stage vaccine candidate with evidence showing some protection against clinical malaria in early field trials (Thera *et al*., 2011).

Despite its importance for merozoite invasion, the biological function of PfAMA1 remained largely unknown until recently. Early genetic studies in *T. gondii* suggest a role for AMA1 in invasion of host cells. Viable *TgAMA1* knockout mutants could not be obtained (Hehl *et al*., 2000) and conditional knockout mutants of *TgAMA1* were severely impaired in host cell invasion (Mital *et al*., 2005). The gene encoding PfAMA1 could not be disrupted in asexual blood stages of *P. falciparum* and other species of *Plasmodium* suggesting it was essential (Triglia *et al*., 2000; Giovannini *et al*., 2011; Bargieri *et al*., 2013). Perhaps the most highly studied aspect of AMA1 is formation of the tight junction, a feature that was initially observed as an electron-dense region at the point of contact between an invading merozoite and the erythrocyte (Aikawa *et al*., 1978). The tight junction is thought to serve as an anchor that together with the parasite actomyosin motor provides the traction needed for merozoites to pull itself into the erythrocyte (Tyler and Boothroyd, 2011; Bargieri *et al*., 2012). The interaction between PfAMA1 and another parasite protein called rhoptry neck protein 2 (RON2) is essential for tight junction formation, which commits the merozoite for invasion (Srinivasan *et al*., 2011b). RON2 is part of a larger RON complex that also contains RON4 and RON5 (Alexander *et al*., 2005; Collins *et al*., 2009; Riglar *et al*., 2011). The RON complex appears to be released from the merozoite's rhoptry organelles prior to penetration and embeds in the erythrocyte surface where it serves as an attachment point for AMA1 (Lamarque *et al*., 2011).

Several lines of evidence support this AMA1–RON2 model of the tight junction. The AMA1–RON2 interaction can be disrupted with small peptides such as RON2L, which competes with native RON2 protein and leads to inhibition of merozoite invasion (Srinivasan *et al*., 2011b). AMA1-binding monoclonal antibodies inhibit merozoite invasion by blocking the AMA1–RON2 interaction. Additionally, the peptide R1 (Harris *et al*., 2005) mimics the structure of the AMA1-binding region of RON2 and as a result blocks merozoite invasion and formation of the tight junction (Vulliez-Le Normand *et al*., 2012).

However, experiments using AMA1 knockout and knockdown mutants in *P. berghei* merozoites and *T. gondii* tachyzoites have suggested that AMA1 plays no role in tight junction formation but rather is important, but not essential, for host cell attachment (Giovannini *et al*., 2011; Bargieri *et al*., 2013). Additionally, these investigators showed that AMA1 is not required for merozoite replication in the erythrocyte and that the reduced multiplication rate they observed of approximately 35% reflects a defect in merozoite entry into the host cell (Bargieri *et al*., 2013).

A dimerizable Cre recombinase (DiCre) technology (Jullien *et al*., 2003) has been adapted for *P. falciparum* and the related apicomplexan parasite *T. gondii* to provide a rapid and efficient method for gene deletion and conditional expression (Andenmatten *et al*., 2013; Collins *et al*., 2013). Using DiCre technology we have constructed a *P. falciparum* parasite in which expression of the PfAMA1 protein is under conditional control resulting in knockdown of protein expression by approximately 80% in a single intraerytrocytic growth cycle. This results in inhibition of merozoite invasion and provides evidence that PfAMA1 is required for successful invasion into erythrocytes.

Results

Conditional regulation of PfAMA1

The gene encoding PfAMA1 is refractory to genetic ablation via conventional knockout strategies (Triglia *et al*., 2000) and consequently we constructed a *P. falciparum* line in which it was placed under conditional regulation. To do this we simultaneously disrupted the endogenous *Pfama1* gene, in the W2mef line by single recombination, with the plasmid pAMA1-loxP allowing complementation with a transfected gene (encodes the antigenically distinct

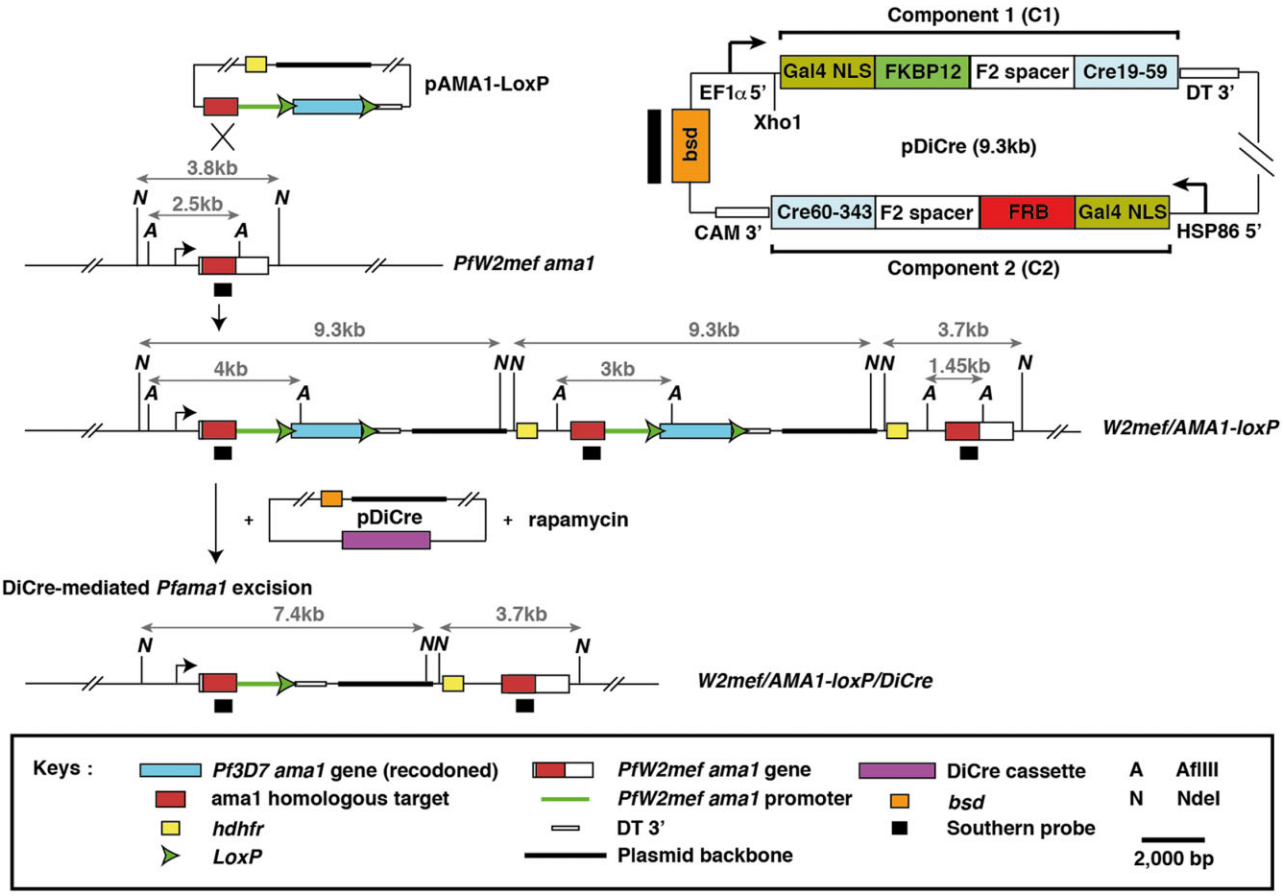

Fig. 1. Schematic for the sequential generation of W2mef/AMA1-loxP and W2mef/AMA1-loxP/DiCre parasites. In the first transfection, the gene for *Pfama1* in W2mef was genetically disrupted and complemented with a codon-altered 3D7 *Pfama1* gene using the pAMA1-loxP plasmid. The main features of pAMA1-loxP are a homologous target sequence for recombination followed by a W2mef promoter sequence and a 'floxed' 3D7 *Pfama1* gene. A *hdhfr* selectable drug cassette, which confers resistance to the antifolate WR99210, was used to select for transfectants. Homologous integration of two tandemly arranged pAMA1-loxP plasmids into the W2mef AMA1 locus resulted in a duplication of the 3D7 *Pfama1* gene. The architecture of the modified locus is shown along with AflIII and NdeI restriction sites used for Southern blot analysis. Sizes of the digested DNA fragments are shown in kilobase (kb). W2mef/AMA1-loxP parasites were cloned by limiting dilution. In the second transfection, DiCre was introduced into a W2mef/AMA1-loxP clone using the pDiCre plasmid. The expression casette of pDiCre is shown in the boxed insert (top right). The N- and C-terminus fragments of Cre recombinase are driven by the bi-directional *P. berghei* EF1α promoter and hsp86 promoter respectively with both Cre fusions placed in a head-to-tail orientation. Transcription termination is modulated by 3′ UTR sequences of *P. berghei* dihydrofolate reductase-thymidylate synthase (DT 3′) and *P. falciparum* calmodulin (CAM 3′) genes. In the DiCre system, Cre recombinase is fused to an F2 linker and either the FKBP12 or FRB sequence to induce dimerization in the presence of rapamycin. We have included a Gal4 nuclear localization signal to target the DiCre fusion proteins to the nucleus once expressed and a *bsd* resistance marker, which confers resistance to blasticidin. The predicted modification of the *Pfama1* locus following DiCre-mediated *Pfama1* excision is shown along with the restriction digest sizes.

3D7 allele) flanked with loxP sites (Fig. 1). The resulting W2mef/AMA1-loxP parasites were cloned by limiting dilution and the clones derived had two copies of the plasmid inserted into the *Pfama1* gene resulting in two functional copies of the 3D7 allele (Figs 1 and 2A, Fig. S1).

In the second step we transfected the plasmid pDiCre, which encodes the two conditionally dimerizable halves of Cre recombinase, into W2mef/AMA1-loxP to derive W2mef/AMA1-loxP/DiCre (Fig. 1). Normally, the DiCre enzyme is inactive hence unable to recombine the loxP sites and excise *Pfama1*. Cre recombinase is activated in the presence of rapamycin as association of the two inactive Cre fragments would occur via FK506-binding protein (FKBP12) and FKBP12-rapamycin-binding (FRB) domain of FRAP (FKBP12-rapamycin-associated protein) (Jullien *et al.*, 2003). Southern blot analysis of W2mef/AMA1-loxP/DiCre parasites confirmed that the pDiCre plasmid was present (Fig. 2B) and that endogenous *Pfama1* gene had been disrupted as expected (Fig. 2A). Two W2mef/AMA1-loxP/DiCre clones were generated (referred to as 2F9 and B4) and used for subsequent analyses. Both 2F9 and B4 transgenic parasites exhibited normal growth rate suggesting there was no deleterious effect of DiCre expression in the absence of rapamycin (data not shown).

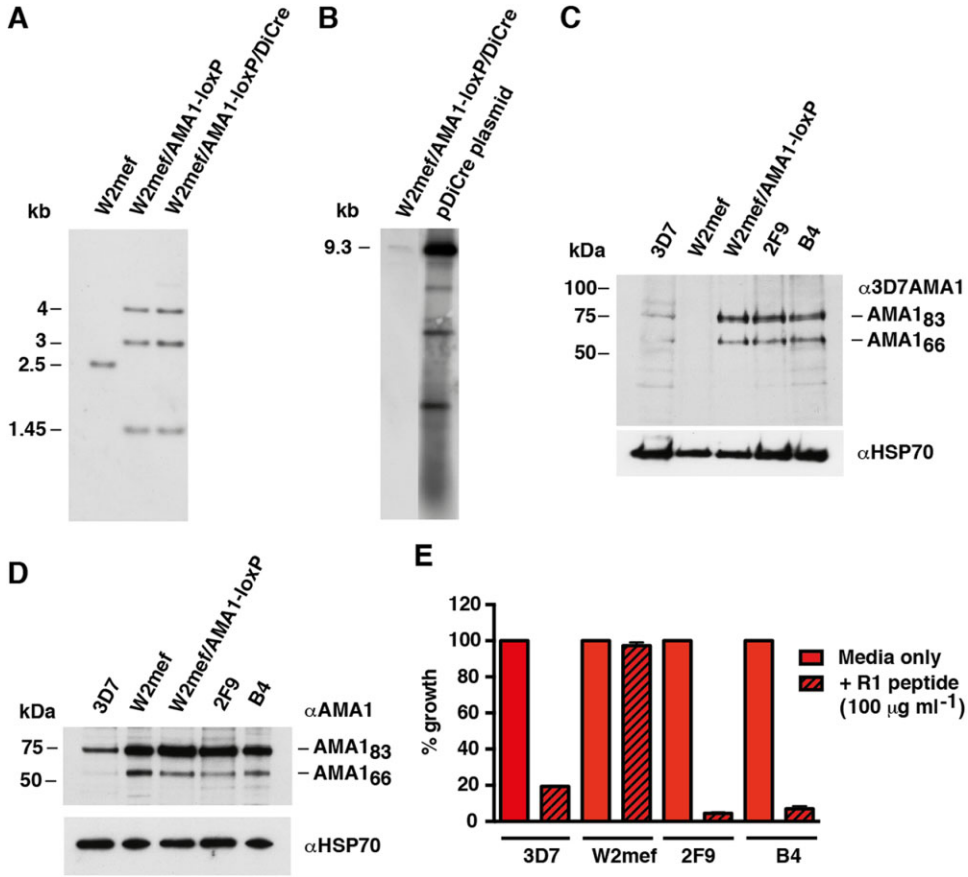

Fig. 2. W2mef/AMA1-loxP and W2mef/AMA1-loxP/DiCre parasites are complemented with the 3D7 AMA1 protein.
A. Southern blot indicates that two copies of pAMA1-loxP have integrated into the W2mef *Pfama1* locus leading to a duplication of the heterologous 3D7 *Pfama1* gene. The 4 and 3 kb AflIII fragments indicate the first and second copy of the full-length integrated plasmid (see Fig. 1). Both 4 and 3 kb signals have equal intensity on the Southern blot, indicating that copy numbers are identical (i.e. 1:1 ratio). The 1.45 kb signal signifies the 3′ end of the modified locus where the second plasmid re-joins the endogenous, disrupted W2mef *Pfama1* gene. This signal is a single copy fragment hence it is used as DNA loading control for each track.
B. Southern blotting using XhoI restriction enzyme confirms the presence of the 9.3 kb full-length pDiCre plasmid in W2mef/AMA1-loxP/DiCre parasites.
C. Immunoblot analysis of late-schizont extracts probed with the specific anti-3D7 AMA1 mAb 3A2 showing the two most abundant forms of AMA1: the 83 kilodalton (kDa) precursor, $AMA1_{83}$ and the 66 kDa processed form, $AMA1_{66}$. The result shows that complementation with 3D7 AMA1 protein has occurred in W2mef/AMA1-loxP and W2mef/AMA1-loxP/DiCre clonal lines (2F9 and B4).
D. A polyclonal PfAMA1 antibody detected PfAMA1 signals from all tracks including parental W2mef confirming the result of the previous immunoblot.
E. Parental and transgenic parasites were grown in media +/– R1 peptide. R1 peptide binds specifically to 3D7 PfAMA1 but not W2mef PfAMA1. Complementation of W2mef/AMA1-loxP/DiCre parasites with a functional 3D7 PfAMA1 protein is evident as R1 peptide significantly inhibited growth of 3D7, 2F9 and B4 parasites but not W2mef ($n = 2$ experiments with each done in triplicate). Error bars indicate standard deviation (SD).

W2mef/AMA1-loxP and W2mef/AMA1-loxP/DiCre parasites express a functional heterologous 3D7 AMA1 protein

Previously, we have generated transgenic *P. falciparum* expressing heterologous *Pfama1* alleles that differ in susceptibility to invasion inhibitory antibodies (Healer *et al.*, 2004). We made use of this strategy to disrupt the endogenous *Pfama1* gene in W2mef while simultaneously complementing loss-of-function with the antigenically distinct 3D7 *Pfama1* allele (Fig. 1). Complementation was confirmed by immunoblot analysis of late-stage schizont stages using a monoclonal antibody specific for the 3D7 PfAMA1 ectodomain and a PfAMA1 rabbit polyclonal antibody. Anti-3D7 AMA1 recognized the full-length and processed forms of AMA1 ($AMA1_{83}$ and $AMA1_{66}$) in W2mef/AMA1-loxP, 2F9 and B4 lines but not in W2mef parental lines (Fig. 2C). In contrast, the polyclonal PfAMA1 antibody detected the protein in transgenic and parental lines showing that W2mef/AMA1-loxP and W2mef/AMA1-loxP/DiCre parasites indeed expressed the 3D7 AMA1 allele (Fig. 2D).

To show that the 3D7 allele of PfAMA1 expressed in the transgenic lines was functional we tested the ability of the 20-residue peptide, R1, to inhibit merozoite invasion into erythrocytes (Harris *et al.*, 2005). The R1 peptide is strain-specific as it recognizes 3D7 AMA1 but has a low affinity for W2mef AMA1. We carried out a flow cytometry (FACS)-based growth assay by incubating 3D7, W2mef, 2F9 and B4 parasites with R1 peptide. In the presence of R1, 3D7 parasite growth was inhibited by approximately 80% while W2mef parasites were not affected (Fig. 2E). In contrast, the growth of 2F9 and B4 that expressed the 3D7 PfAMA1 was inhibited by 90–95% in the presence of R1 consistent with these transgenic parasites expressing functional 3D7 AMA1 protein (Fig. 2E).

DiCre-mediated excision of the PfAMA1 gene

To determine the efficiency of DiCre-mediated excision of the inserted *Pfama1* genes, we first determined the off-target effect of rapamycin on parasite growth (Fig. S2A–C). Accordingly, we used rapamycin at 0.1 or 0.2 μM in subsequent experiments as W2mef and W2mef/AMA1-loxP parasites grew normally at these concentrations. Next, B4 and 2F9 parasites were synchronized and incubated with either 0.1% DMSO or 0.1 μM rapamycin for 48, 96, 144 or 192 h. Genomic DNA was extracted from parasites and analysed by Southern blot to determine the level of DiCre-mediated excision of *Pfama1*. A single-copy 3.7 kb band corresponding to the 3′ end of the plasmid pAMA1-loxP crossover was used as loading control (Figs 1 and 3A). Rapamycin-induced excision of *Pfama1* was demonstrated by a shift from a band of 9.3 kb to 7.4 kb. The percentage of excision varied from 70% to 92% as quantified by densitometry in both B4 and 2F9 parasites after 48 h with rapamycin (Fig. 3B and C). In each of the subsequent time points, there was excision of *Pfama1* to the same extent of approximately 80% in both B4 and 2F9 parasites. The lack of an additive effect in terms of the excision rate was unexpected since continuous expression of DiCre should result in all of the *Pfama1* genes being deleted. This was most likely because expression of DiCre activity was not sufficient to excise all *Pfama1* copies within a single intraerythrocytic growth cycle and approximately 20% expressed sufficient protein to invade and survive.

Therefore we determined when DiCre activity could be detected within one intraerythrocytic growth cycle by Southern blot analysis. Excision of *Pfama1* was first detected at 30 h post incubation with rapamycin (Fig. 3D and E). This was consistent with the EF1α bi-directional promoter not being active during ring-stage of the parasite life cycle (Fig. 1).

Excision of Pfama1 results in decreased PfAMA1 expression

The amount of *Pfama1* gene excision in the B4 and 2F9 populations was between 70–92% and we next determined the corresponding level of PfAMA1 protein expression when Cre recombinase activity was induced by rapamycin. Schizont-stage parasites were analysed by immunoblot using α-3D7 AMA1 antibody. There was approximately 81% knockdown of AMA1 protein levels across the four time points when compared with untreated parasites (Fig. 4A–C). Expression of other invasion proteins such as PfRh4, RON4 and EBA175 was unaffected (Fig. 4D). This level of PfAMA1 protein knockdown correlated with the level of *Pfama1* gene excision mediated by DiCre.

We next determined the level of PfAMA1 protein expression using immunomicroscopy of untreated and rapamycin-treated late stage schizonts. Parasites were treated with rapamycin or DMSO for 48 h. This revealed a gradient of PfAMA1 signal intensities ranging from high levels to no detectable PfAMA1 for both conditions (Fig. 4E). Parasites not treated with rapamycin also displayed some variation in PfAMA1 signal intensity dependent upon the maturity of the schizonts (data not shown). To impartially determine if rapamycin treatment resulted in reduced PfAMA1 expression, the average pixel intensity within a 70 pixel diameter region encompassing the schizonts was measured. Only parasites positive for the schizont-stage marker merozoite surface protein 1 (MSP1) were counted because the timing of MSP1 protein expression is activated just before that of PfAMA1 (PlasmoDB, http://plasmodb.org/plasmo). A histogram of the pixel intensities confirmed that rapamycin treatment resulted in less than half as many strongly staining AMA1-positive parasites (+ rapamycin: 21 parasites; – rapamycin: 56 parasites) and more medium to weakly staining parasites (+ rapamycin: 103 parasites; – rapamycin: 68 parasites) (Fig. 4F). Of 124 schizonts observed, 83% were medium to weakly staining AMA1-positive parasites in the rapamycin treatment group compared with 55% in non-treated group. The shift towards decreased PfAMA1 staining following rapamycin treatment suggests deletion of *Pfama1* was directly contributing to reduction of PfAMA1. Microscopy of schizonts with reduced PfAMA1 showed that all of the merozoite microneme organelles within any particular parasite cell were evenly stained indicating that the extent of PfAMA1 knockdown was uniform between daughter merozoites (Fig. 4E).

AMA1 knockdown leads to growth inhibition of W2mef/AMA1-loxP/DiCre parasites

To determine if knockdown of PfAMA1 induced by DiCre expression affected parasite growth and invasion, we

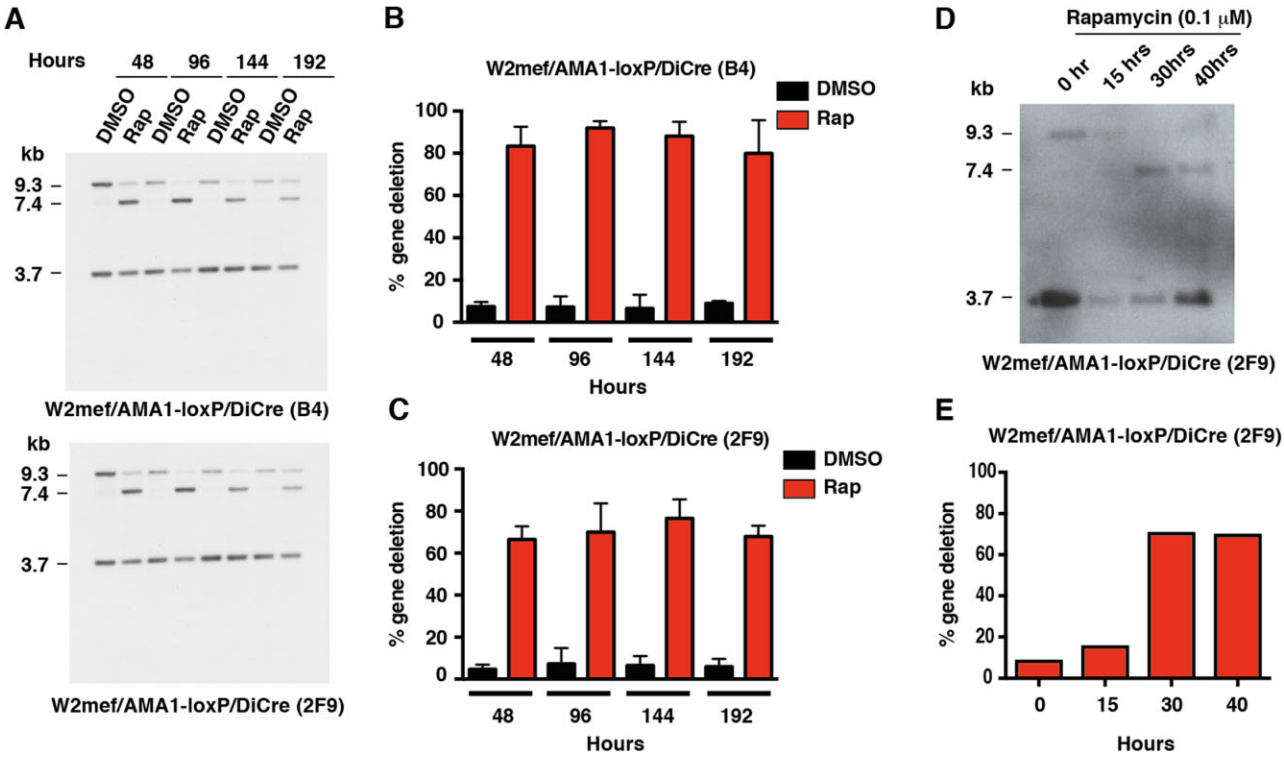

Fig. 3. Efficient DiCre-mediated deletion of *Pfama1* within one cycle of intraerythrocytic growth.
A. Representative Southern blots showing efficient DiCre-mediated excision of *Pfama1* in clones B4 (top) and 2F9 (bottom) over four time points each corresponding to an intraerythrocytic growth cycle. Highly synchronized ring-stage parasites were split into eight dishes. Half were treated with 0.1 μM rapamycin (Rap) while the remaining dishes were treated with 0.1% DMSO as the vehicle control. Genomic DNA was extracted for every treatment pair (Rap and DMSO) after 48, 96, 144 and 192 h when parasites were at the late-schizont stage. Southern blotting of genomic DNA digested with NdeI detected three fragments in each track. An intact *Pfama1* gene is represented by the 'non-excised' 9.3 kb fragment while deletion of *Pfama1* gene is represented by the 'excised' 7.4 kb fragment. An additional 3.7 kb fragment corresponds to the single-copy 3′ end of the pAMA1-loxP integration event and acts as a measure for DNA loading in each track. At each time point, rapamycin treatment resulted in a higher proportion of 'excised' fragments compared with DMSO treatment, which showed almost non-existential background DNA recombination ($n = 2$).
B. Densitometric quantification reveals *Pfama1* excision rate ranges from 70–92% at each time point for B4 parasites. This was determined by the ratio of the intensity of the 'excised' fragment to total intensity ('excised' and 'non-excised' fragments) in each track, normalized against DNA loading ($n = 2$). Error bars indicate SD.
C. Similar analysis on 2F9 parasites results in equally efficient excision of *Pfama1* ($n = 2$). Error bars indicate SD.
D. A Southern blot time-course on 2F9 parasites reveals that the 'excised' fragment was first detected at 30 h after addition of rapamycin. DiCre-mediated excision of *Pfama1* occurs during mid-to-late trophozoite stage.
E. Densitometric analysis of the Southern blot time-course indicates that a significant increase in *Pfama1* deletion occurred between 15 and 30 h post rapamycin treatment.

measured the ability of W2mef/AMA1-loxP/DiCre cloned parasite lines (2F9 and B4) to multiply in the presence of rapamycin. Both 2F9 and B4 parasites showed a reduction in growth in a dose-dependent manner to a maximum reduction of 40% over 72 h (Fig. 5A and B). We monitored growth of rapamycin-treated W2mef/AMA1-loxP/DiCre parasites through intraerythrocytic development and it was found to be the same as non-rapamycin treated parasites supporting the idea that loss of PfAMA1 function was affecting merozoite invasion (Fig. S3A). Furthermore, parasite growth was monitored for extended periods under rapamycin treatment. Rapamycin treatment had no effect on W2mef/AMA1-loxP parasites, which lack DiCre expression (Fig. 5C). In contrast, rapamycin-treated W2mef/AMA1-loxP/DiCre parasites had greatly reduced growth relative to untreated parasites (Fig. 5D and E). These results showed that PfAMA1 was required for normal growth of *P. falciparum*.

PfAMA1 is required for invasion of erythrocytes by merozoites

We showed that PfAMA1 function in *P. falciparum* was required for growth. To determine if this was due to an essential role in invasion, purified merozoites of 2F9 and B4 parasites were tested for their ability to invade erythrocytes (Boyle *et al.*, 2010). PfAMA1 protein knockdown in the purified merozoites was confirmed by immunoblot analysis that showed they expressed 60–80% less protein following rapamycin treatment (data not shown). In four

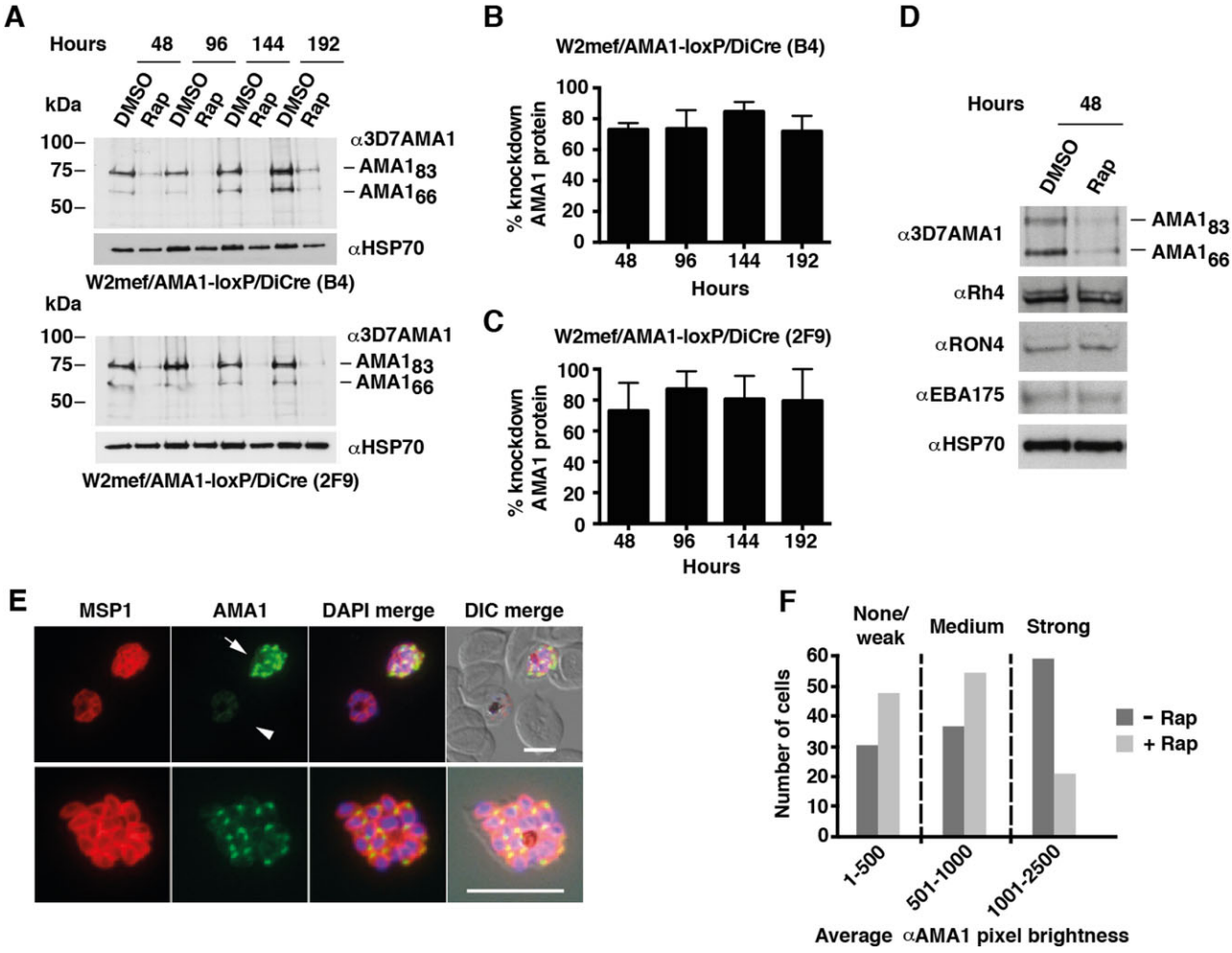

Fig. 4. Rapamycin strongly and specifically depletes PfAMA1 expression in late stage parasites.
A. Representative immunoblots show significantly decreased PfAMA1 expression following rapamycin treatment in B4 (top two panels) and 2F9 (bottom two panels) parasites over four time points. A monoclonal antibody specific for 3D7 AMA1 was used, which detected both the unprocessed 83 kDa and processed 66 kDa PfAMA1. Anti-HSP70 was used as loading control.
B and C. By using densitometry quantification, PfAMA1 knockdown was estimated at an average of 81% for both parasite lines and in each of the four time points ($n = 2$). Error bars indicate SD.
D. Immunoblot analysis indicates that expression of other rhoptry and micronemal proteins such as PfRh4, PfRON4 and PfEBA175 were not reduced by rapamycin treatment.
E. Schizonts of rapamycin-treated parasites were dual labelled with anti-MSP1 (red) and anti-PfAMA1 (green) to show reduction in PfAMA1 expression. Schizonts displaying a gradient of high (arrow, top row), medium (bottom row) and low (arrowhead, top row) levels of PfAMA1 expression were observed. Scale bar is 5 μm.
F. Histogram of pixel brightness of PfAMA1 antibody-labelled parasites, categorized into three groups: strong, medium and weak/none. Average pixel intensity for PfAMA1 was measured within a 70 pixel diameter surrounding the parasite and only MSP1-positive schizont stages were selected.

independent experiments for cloned lines 2F9 and B4, rapamycin-mediated PfAMA1 knockdown resulted in merozoite invasion between 43–85% of untreated control (Fig. 5F). On average, merozoites invaded 37% less effectively following rapamycin treatment for 48 h (Fig. 5G) and this was in agreement with the growth inhibition rate determined previously. Therefore PfAMA1 is required for invasion of *P. falciparum* merozoites into erythrocytes.

Real time imaging of rapamycin-treated W2mef/AMA1-loxP/DiCre merozoites shows a reduced ability to invade

Rapamycin-induced *Pfama1* deletion resulted in a significant reduction of merozoite invasion and we used real time imaging to investigate the mechanistic defect. Live W2mef/AMA1-loxP/DiCre parasites were imaged under normal growth conditions following treatment with or

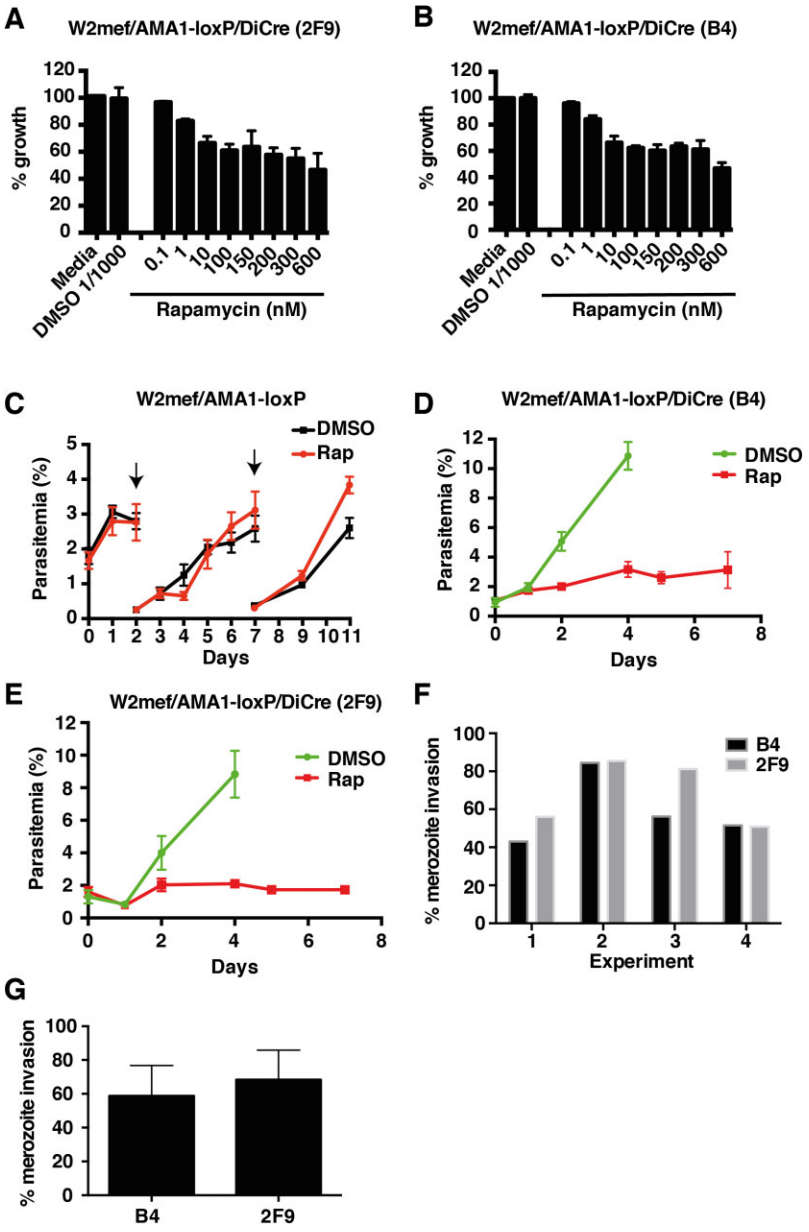

Fig. 5. PfAMA1 knockdown leads to substantial growth inhibition due to decreased merozoite invasion.
A and B. FACS-based growth assays show a dose-dependent growth inhibition of 2F9 and B4 parasites in the presence of rapamycin. At 0.1 μM rapamycin (non-inhibitory to wild type growth), DiCre-mediated knockdown of PfAMA1 resulted in 40% growth inhibition ($n = 3$; triplicate experiments). Error bars indicate SD.
C. Rapamycin does not affect W2mef/AMA1-loxP parasite growth as both DMSO- and rapamycin-treated parasites expanded normally. Arrows denote splitting of parasites ($n = 2$; triplicate experiments). A representative experiment is shown. Error bars indicate SD.
D and E. B4 and 2F9 parasites do not expand normally over the course of a week upon rapamycin-mediated PfAMA1 knockdown. DMSO-treated parasites grew normally and parasitemia were recorded up to four days ($n = 2$ in triplicate). A representative experiment is shown and similar results were obtained for 2F9 parasites. Error bars indicate SD.
F. Rapamycin-mediated PfAMA1 knockdown results in reduced merozoite invasion of erythrocytes. Invasion assays were performed using purified merozoites incubated with either 0.1 μM rapamycin or 0.1% DMSO v/v. In four independent experiments, rapamycin-treated 2F9 and B4 merozoites invaded at 43–85% of DMSO-treated merozoites.
G. On average, rapamycin treatment leads to 37% invasion inhibition in both 2F9 and B4 merozoites ($n = 4$; triplicate experiments). Error bars indicate SD.

without rapamycin. Late-stage schizonts were imaged by time-lapse microscopy for periods of 15–30 min. Following schizont rupture, untreated W2mef/AMA1-loxP parasites merozoites behaved similarly to wild type merozoites in that those that contacted erythrocytes deformed their target cells for several seconds before penetration (Fig. 6A) (Gilson and Crabb, 2009). Invasion itself lasted approximately 10 s after which the erythrocyte underwent echinocytosis 30–60 s later. Echinocytosis appears to be caused by dehydration of the host cell (Tiffert *et al.*, 2005) and took an average of 376 s for recovery. During the recovery process the merozoite could be observed transforming into an amoeboid ring stage parasite (Gruring *et al.*, 2011; Riglar *et al.*, 2011). Of 38 attempted invasions observed for untreated merozoites 35 appeared successful and 3 failed (Fig. 6D). In one of the failed invasions the merozoite deformed the erythrocyte, triggered its echinocytosis but failed to penetrate and remained attached to the outside of the erythrocyte. In the other two failed invasions the merozoites penetrated, triggered echinocytosis but then reversed out of the invasion site back onto the outside of the erythrocyte.

Following rapamycin treatment and knockdown of PfAMA1 expression the proportion of merozoites failing to productively invade and transform into a ring stage parasite increased to approximately 40% (Fig. 6D). The merozoites that failed to invade fell into two groups: first, those that failed to penetrate, caused echinocytosis and

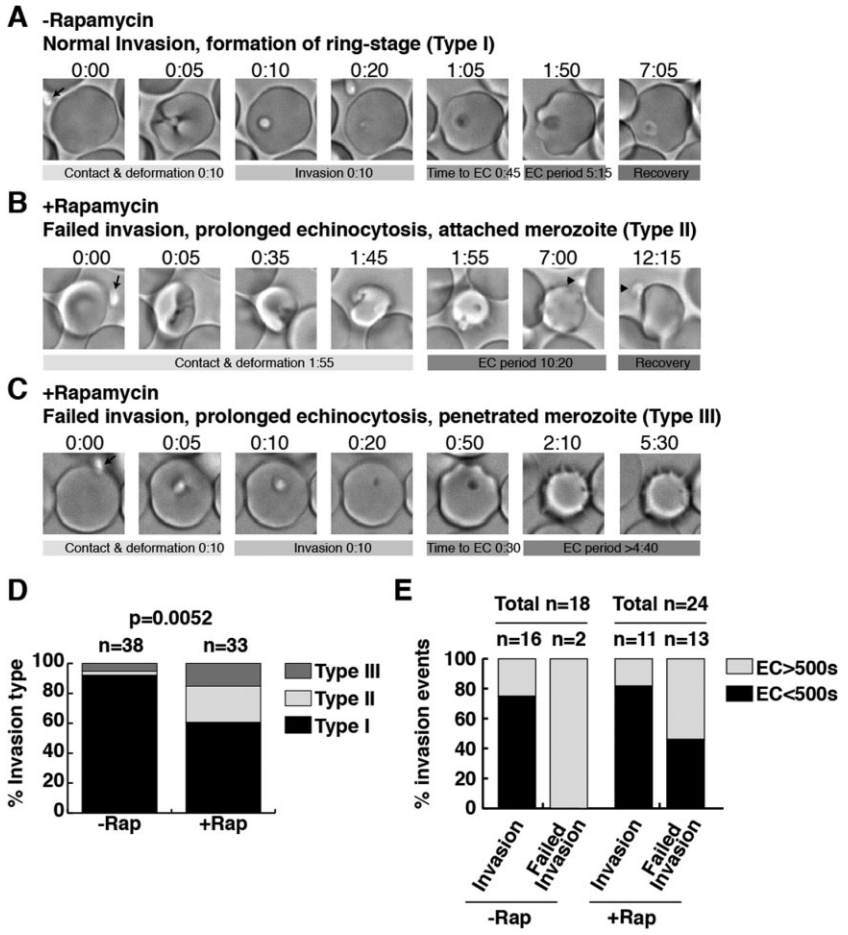

Fig. 6. Rapamycin induction of DiCre results in increased merozoites that cannot invade erythrocytes.
A. Selected still images from a video sequence showing an untreated merozoite (arrow) successfully invading an erythrocyte (Type I invasion). Time is shown in minutes and seconds.
B. Rapamycin-treated merozoite (arrow) that deforms but cannot invade its target erythrocyte. The merozoite triggers echinocytosis and remains attached to its target erythrocyte (arrowheads) (Type II invasion).
C. Rapamycin-treated merozoite (arrow) that penetrates but fails to reseal its target erythrocyte and does not develop into a ring-stage parasite (Type III invasion).
D. The ratio of successful invasion (Type I) versus unsuccessful invasion (Type II and III) decreases in the presence of rapamycin ($P = 0.0052$, Fisher's exact test).
E. Rapamycin treatment results in a greater percentage of failed invasion events. About 60% of the failed invasion events were due to prolonged echinocytosis (EC) periods of > 500 s (s). Note that the total number of events (n) for +/– Rap is not the same in D and E because the echinocytosis period could not be ascertained for every invasion event.

remained attached (Fig. 6B) and second, those that penetrated, triggered echinocytosis but failed to produce a ring (Fig. 6C). In the latter group some merozoites exited after penetration whilst others remained internal. In many of the failed invasions the target erythrocyte remained an echinocyte for a greatly extended period compared with successful invasions suggesting a failure to reseal the erythrocyte surface following penetration or attempted penetration (Fig. 6E). In the case of the successful invasions they generally had an echinocytosis period less than 500 s (Fig. 6E). About 60% of the failed invasion events for rapamycin-treated merozoites were characterized by echinocytosis periods more than 500 s consistent with the idea that they had a defect in resealing the invaded erythrocyte (Fig. 6E).

Discussion

AMA1 is one of the most intensely studied apicomplexan ligands and much data has strongly implied an obligatory role for this protein in the invasion of *Plasmodium* merozoites into host erythrocytes. Notably, despite efforts by numerous groups using different systems, it has not proven possible to permanently delete the gene encoding AMA1 in a range of *Plasmodium* species (Triglia *et al*., 2000; Bargieri *et al*., 2013). While gene disruption has proved impossible, studies using transgenic complementation approaches and inhibition of endogenous PfAMA1 using the R1 peptide have been successful (Healer *et al*., 2004; Drew *et al*., 2012). These have provided a system to test the function of PfAMA1 by inserting specific mutations and through this added additional evidence that this protein is required for merozoite invasion (Leykauf *et al*., 2010). Together, the data reported in this study shows that blood-stage growth is substantially impeded, probably prevented altogether, in the absence of AMA1.

Mechanistically, it is known that AMA1 binds to another parasite-encoded protein RON2 that is part of a parasite complex injected into the host cell membrane at the pre-invasion stage thereby functioning as an erythrocyte-surface receptor (Besteiro *et al*., 2009; Cao *et al*., 2009; Richard *et al*., 2010; Lamarque *et al*., 2011; Tonkin *et al*., 2011; Tyler and Boothroyd, 2011). Indeed, during invasion by *P. falciparum* merozoites PfAMA1 can be observed forming a ring around the surface that moves with the tight junction together with the RON complex consistent with it

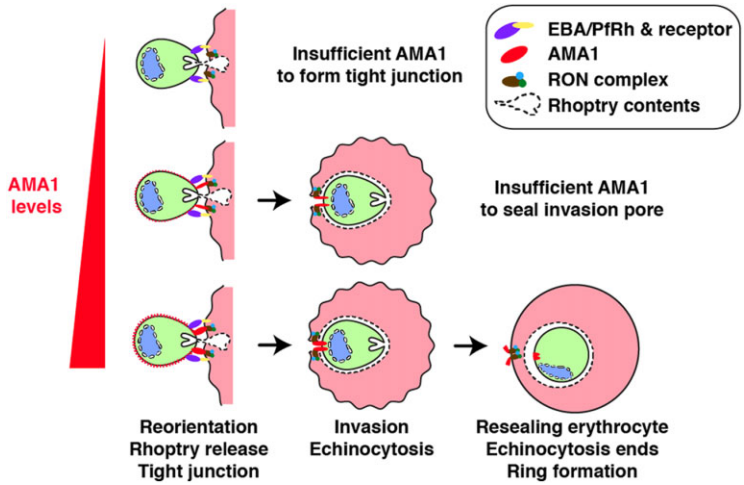

Fig. 7. Model showing the role of AMA1 during merozoite invasion into erythrocytes. AMA1 is implicated in the initial stages of merozoite invasion, including rhoptry secretion into erythrocytes, tight junction formation (Riglar *et al*., 2011) and possibly apical reorientation (Mitchell *et al*., 2004) although this has recently been refuted (Srinivasan *et al*., 2011a). The tight junction serves as an anchor for the myosin-dependent penetration of the merozoite (Gonzalez *et al*., 2009). The penetration step coincides with the formation of the parasitophorous vacuole (PV) made up of rhoptry contents and a 5–10 min period of echinocytosis. Once the merozoite has completed its entry, the PV pinches off the erythrocyte membrane, the erythrocyte re-seals and reverts back to its normal shape (Gilson and Crabb, 2009). Expression of AMA1 is in excess in wild type parasites and as the level of AMA1 reduces, less efficient re-sealing of the erythrocyte membrane occurs. This is shown by prolonged echinocytosis in which there is sufficient AMA1 to form a penetrative tight junction but not a re-sealing tight junction. Further reduction of AMA1 leads to the inability to form tight junction and merozoite remains attached but do not penetrate the erythrocyte.

binding directly to the RON complex and playing an essential role in this process (Riglar *et al*., 2011). Using different agents (antibodies and peptides) that block the AMA1–RON2 interaction, much data has been generated in both *Plasmodium* merozoites and *Toxoplasma* tachyzoites that suggests this interaction is absolutely required for the establishment of the tight junction and hence is essential for invasion (Hehl *et al*., 2000; Harris *et al*., 2005; Richard *et al*., 2010; Lamarque *et al*., 2011; Riglar *et al*., 2011; Srinivasan *et al*., 2011b). These data are of course consistent with the inability to disrupt the *Plasmodium ama1* gene under circumstances that require parasite maintenance in blood-stage culture.

Given the data described above, it was surprising that deletion of the *ama1* gene, using the conditional FLP/*FRT* system in the rodent malaria parasite *P. berghei*, suggested that AMA1 was not essential for tight-junction formation or indeed for invasion (Bargieri *et al*., 2013). Hence, uncertainty remains about the function of AMA1, especially its role in the invasion of erythrocytes by *Plasmodium* merozoites. In this paper, we sought to further address the issue employing a different conditional system and using *in vitro* cultured *P. falciparum* parasites. We placed *Pfama1* under conditional control in *P. falciparum* merozoites using DiCre and an allelic replacement strategy that allows excision of the functional gene and concordantly decreased PfAMA1 expression in the parasite population.

The imperfect nature of the genetic deletion event using this system (~ 80%), and the fact that the timing of deletion is post-DNA replication (because the recombinase is under the control of a trophozoite-stage promoter) means that many of the schizonts will include a mixture of merozoites that are genetically null and wild type for the *Pfama1* gene. In such circumstances we predicted the PfAMA1 protein that is synthesized in these schizonts should get distributed evenly to all the merozoites as microneme biogenesis precedes parasite segmentation. Indeed, our IFA data were consistent with the even AMA1 staining in each merozoites within schizonts that ranged in brightness from very dull to bright. Hence, although the genetic deletion is around 80%, the merozoites in the rapamycin population have a range of AMA1 levels from none, very low and close to normal (see Fig. 7).

Our PfAMA1-deficient merozoite population was unable to invade erythrocytes as effectively as wild type parasites. Real time imaging of merozoite invasion has shown that the 'non-invaders' can adhere to the erythrocyte and cause characteristic deformations that precede activation of invasion. This is similar to the invasion phenotype observed following treatment with the R1 peptide (Leykauf *et al*., 2010). Occupation of AMA1's RON2 binding pocket by the R1 peptide prevents tight junction formation but not echinocytosis, an event that is probably triggered by rhoptry release occurring independently of tight junction formation by permeabilizing the erythrocyte

surface (Gilson and Crabb, 2009). Due to the phenotypic similarity to R1 treatment it suggests that the rapamycin-treated merozoites that failed to penetrate the host cell probably have none or very small amounts of PfAMA1 expression (Fig. 7). Conversely, the rapamycin-treated merozoites that penetrate their target erythrocytes probably have enough PfAMA1 to form a tight junction. However, the merozoites that failed to seal the erythrocyte behind them, and which in some cases exit via the invasion pocket, probably lack sufficient PfAMA1 to enable the tight junction to operate efficiently to pinch off the parasitophorous vacuole and reseal the erythrocyte plasma membrane (Fig. 7).

Interestingly, half of the rapamycin-treated merozoites that successfully invaded have greatly extended echinocytosis periods consistent with these parasites having a less efficient tight junction. This implies that PfAMA1 is in excess in normal parasites and that as its level is reduced less efficient resealing occurs. Once the PfAMA1 levels are reduced below a threshold a penetrative tight junction can still be formed but its organization is insufficient for resealing of the erythrocyte. Further reduction in PfAMA1 leads to no tight junction formation and therefore no penetration.

As mentioned above, in a separate study by Bargieri *et al*. conditional *ama1* gene knockout mutants have been obtained in *P. berghei* and *T. gondii* using a conditional FLP/*FRT* system (Bargieri *et al*., 2013). While orthologues and/or paralogues of AMA1 have been identified that may function in its absence in *Plasmodium* sporozoites (e.g. MAEBL) or *T. gondii* tachyzoites (Poukchanski *et al*., 2013) there are no obvious candidates expressed in *Plasmodium* merozoites that may complement AMA1 function at this stage in the life cycle. Since these merozoites could still invade despite not having any detectable AMA1 these authors concluded that AMA1 was not essential for tight junction formation or invasion (Bargieri *et al*., 2013), in contrast to our data in this paper. However, another possible interpretation of their data is that these *P. berghei* merozoites may possess small amounts of AMA1 protein; due to incomplete gene excision in a given hepatic schizont. Hence, with respect to *Plasmodium* merozoite invasion of erythrocytes, it is possible that the results of our study and that of Bargieri *et al*. are consistent (Bargieri *et al*., 2013).

In conclusion, our data adds direct functional evidence to an already very strong existing case that AMA1 is essential for *Plasmodium* merozoite invasion and that it operates by promoting tight-junction formation and functioning. Moreover, intermediate levels of AMA1 expression in some of our merozoite mutants may have revealed another role for AMA1 in the re-sealing of the tight-junction following invasion. The latter clearly requires more investigation.

Experimental procedures

Cloning of DNA constructs

Table S1 contains a list of all primers used in this study. pAMA1-loxP was generated by modifying pCC1AMA1TP.1, an intermediate construct from a previous study (Drew *et al*., 2012). pCC1AMA1TP.1 already contained the W2mef *Pfama1* target sequence and W2mef *Pfama1* promoter. A full-length, codon-optimized 3D7 *Pfama1* sequence flanked by a pair of loxP sites arranged as direct repeats was synthesized by Life Technologies (USA). The 3D7 *Pfama1* synthetic fragment was subsequently cloned in pCC1AMA1TP.1 using KpnI and PstI to produce the final construct, pAMA1-loxP. The DiCre components (boxed insert in Fig. 1) were synthesized by Life Technologies (USA). A nuclear localization signal (NLS) comprising the first 74 residues of yeast Gal4 (Wittayacom *et al*., 2010) was included in the N-terminal region of each component. In component 1 (C1), NLS is followed by FKBP12, the F2 spacer and residues 19–59 of Cre recombinase (Jullien *et al*., 2003). C1 is flanked by XhoI/PstI restriction sites. Component 2 (C2) is composed of NLS, FRB, F2 spacer and residues 60–343 of Cre recombinase. C2 is flanked by XmaI/SpeI restriction sites. The vector to express the DiCre components was made based on pEF-Luc-GFP-DD29 (de Azevedo *et al*., 2012). The selectable marker hDHFR was replaced with blasticidin S-deaminase (BSD), which was retrieved from pCC4 (Maier *et al*., 2008), then digested with BamHI/HindIII and cloned in pEF-Luc-GFP-DD29 generating pEF-Luc-GFP-DD29-BSD. *P. berghei* hDHFR 3′ UTR (DT 3′) was PCR amplified from pCC1 (Maier *et al*., 2008) with primers F-PbDT3-Pst and R-PbDT3-Mlu (Table S1), digested with PstI/MluI and cloned in pEF-Luc-GFP-DD29-BSD, generating pEF-Luc-DT3. C1 was cloned in XhoI/PstI sites of pEF-Luc-DT3, generating pEF-C1-DT3. Heat shock protein 86 promoter (HSP86 5′) was PCR amplified from pCC1 (Maier *et al*., 2008) with primers F-HSP86-Mlu and R-HSP86-Xma, digested with MluI/XmaI and cloned in pEF-C1-DT3, generating pEF-C1-DT3-HSP. C2 was digested with XmaI/SpeI and cloned in pEF-C1-DT3-HSP, generating the final construct pDiCre (Fig. 1).

Parasite cultures and transfections

Asexual blood stage cultures of *P. falciparum* 3D7 and W2mef clones were maintained in human O^+ erythrocytes using standard conditions (Maier *et al*., 2008). The use of human erythrocytes for parasite culturing was approved by the Walter and Eliza Hall Human Research Ethics Committee (ethics number 86/17) and an Australian Red Cross Blood Service Agreement (11-09VIC-01). Transfection of W2mef parasites was as described (Crabb *et al*., 2004). Briefly, synchronized ring-stage parasites at 5–8% parasitemia were electroporated with 100 μg of plasmid. Stable transformants of W2mef/AMA1-loxP were selected on the antifolate drug, WR99210 (2.5 nM). Transfection of W2mef/AMA1-loxP parasites with pDiCre was performed using the Nucleofector® Technology (Lonza) (Janse *et al*., 2006). Mature schizonts were isolated from a synchronized culture using 60% Percoll solution (GE Healthcare). Purified schizonts were transfected by electroporation with 50 μg of pDiCre using Amaxa Nucleofactor® device (Lonza), Basic Parasite Nucleofactor® Kit 1 (Lonza) and program U33. W2mef/AMA1-loxP/DiCre parasites were selected using blasticidin (2.5 μg ml^{-1}, Invitrogen) and cultured in a shaking incubator to improve parasite growth post

transfection (Allen and Kirk, 2010). Two W2mef/AMA1-loxP/DiCre clones, 2F9 and B4, were isolated by limiting dilution and used for subsequent analyses.

Induction of DNA recombination

Rapamycin was obtained from LC Laboratories (USA) and solubilized in DMSO at 2.73 mM. To induce dimerization of DiCre, 0.1 or 0.2 μM rapamycin was added to W2mef/AMA1-loxP/DiCre clones with a final concentration of 0.1% DMSO in all cases.

DNA analysis by Southern blot

Parasite genomic DNA was isolated using standard phenol/chloroform extraction methods (Sambrook *et al*., 1989). Two digoxigenin (DIG)-labelled probes were synthesized using PCR DIG Probe Synthesis Kit (Roche). The W2mef *Pfama1* targeting sequence probe was amplified with primers mo493 and mo492 using pAMA1-loxP plasmid as template (Table S1). As for the *bsd* probe, pDiCe plasmid was used as the PCR template along with primers aw317 and aw318 (Table S1). For Southern blots genomic DNA was digested to completion with AflIII (for pAMA1-loxP integration analysis), NdeI (for *Pfama1* excision analysis) or XhoI (to verify the presence of pDiCre), then separated on a 0.8% agarose gel and transferred to Hybond N + nylon membrane (GE Healthcare). Detection was performed using the DIG Easy Hyb kit (Roche) according to manufacturer's protocol. Quantification of the Southern blot signals was performed using Quantity One 1-D Analysis Software (Bio-Rad).

Immunoblot

Synchronous mature schizonts were harvested and suspended in 0.15% saponin. Saponin pellet was solubilized in SDS sample buffer and separated by SDS-PAGE. Immunoblots of AMA1 were analysed using monoclonal antibody (mAb) 3A2, which specifically recognizes 3D7 AMA1. Other antibodies used in this study include a rabbit polyclonal AMA1 antibody R190, polyclonal antibody against EBA-175 R1179, PfRh4 mAb 2E8 and mAb against PfRON4. Anti-HSP70 polyclonal antibody was used as loading control.

Intracellular parasite growth assay

Parasite growth assays were performed as previously described (Wilson *et al*., 2010). Synchronized ring-stage parasites were plated in triplicates (50 μl) at 1% parasitemia and 1% haematocrit. Rapamycin or DMSO was added with a 1 in 10 dilution to assess growth inhibition over one cycle of intraerythrocytic growth. Parasites were cultured for 72 h through to the next cycle when most parasites progressed to mature trophozoites. Parasites were stained with 10 μg ml^{-1} ethidium bromide (EtBr; Bio-Rad) for an hour and parasitemia was assessed by flow cytometry. The R1 peptide growth assay used the same protocol and R1 peptide was added at 100 μg ml^{-1}.

Merozoite invasion inhibition assay

Merozoites were purified based on an established method (Boyle *et al*., 2010). Highly synchronized ring-stage parasite of clones 2F9 and B4 (typical culture volume of 200 ml each, > 5% parasitemia and 2–3% haematocrit) were split and grown in 0.1 μM rapamycin or 0.1% DMSO v/v until they were late schizonts. Schizonts were isolated from uninfected erythrocytes with a MAC magnet separation column (Macs; Miltenyi Biotech). Purified schizonts were incubated with 10 μM of the cysteine protease inhibitor E64 to prevent schizont ruptures. After 5–6 h of incubation, schizont pellets were passaged through a 1.2 μm syringe filter (Acrodisc; 32 mm; Pall). Filtrate containing purified merozoites was plated out in triplicates (10 μl each well, topped up with media to total 50 μl) with the addition of 0.5% uninfected erythrocytes. Plates were agitated for 10 min. In the next cycle when parasites progressed to become mature trophozoite-stage, parasitemia was assessed by flow cytometry as described earlier. Remaining purified merozoites not used in this assay were pelleted and solubilized in SDS sample buffer for Western blot analysis. Also, purified merozoites were retrospectively quantified using CountBright® absolute counting beads (Life Technologies) to ensure that the number of purified merozoites added at the start of the invasion assays was the same between rapamycin treament and DMSO treatment.

An alternative method was used for measuring invasion inhibition following multiple cycles of growth in the presence of rapamycin. 250 μl of sorbitol-synchronized, ring-stage 2F9 clone were cultured in a 96-well microtitre plate at 1% hematocrit. Samples were plated in triplicate and treated with either DMSO or rapamycin. 50 μl of samples from each well were removed, fixed with 0.25% glutaraldehyde in 1× phosphate buffered saline (PBS) and then incubated with 100 μl of SYBR Green I (Invitrogen) for 15 min. Cells were finally resuspended in PBS for flow cytometry. Samples were collected on day 0 to day 7 with each sample about 24 h apart. Initial gating was carried out with wild type 3D7 parasites and by comparing to Giemsa smears, this method accurately distinguishes ring-stage from late-stage parasites.

Microscopy

Air-dried smears of infected erythrocytes were fixed in ice-cold methanol for 5 min and then blocked for 1 h in PBS with 1% casein. Parasites were probed with rabbit polyclonal IgG to MSP1–19 (60 μg ml^{-1}) and mouse monoclonal IgG to PfAMA1 (2H4, 100 μg ml^{-1}) in blocking buffer for 1 h. After briefly washing twice in PBS with 0.05% Tween 20 and once in PBS, the parasites were probed in goat anti-rabbit Alexa 568 and anti-mouse Alexa 488 (both at 1 in 2000, Invitrogen) for 1 h. After washing as above, the parasites were mounted in Vectashield with DAPI (Vector). Images were taken on a Zeiss AxioObserver with a 100× oil lens and manipulated in ImageJ. For measuring PfAMA1 intensity all images were captured with the same exposure time and adjusted to the same minimum and maximum threshold settings of 160 and 2012 respectively. A 70-pixel diameter circle was drawn around each schizont and the minimum, average and maximum pixel intensities were acquired in ImageJ and manipulated in Microsoft Excel and Prism (Graphpad Software).

Real-time imaging

Late stage W2mef/AMA1-loxP/DiCre (2F9 and B4) schizonts (2 ml) at 0.16% hematocrit were settled onto a 35 mm Fluorodish (World Precision Instruments) and imaged on an inverted Zeiss

AxioObserver microscope in brightfield. The sample chamber was heated to 37°C and supplied with a humidified 1% O_2, 5% CO_2 and 94% N_2 atmosphere.

Acknowledgements

We thank the Red Cross Blood Service (Melbourne, Australia) for supply of red blood cells as well as serum and the Walter and Eliza Hall Institute of Medical Research Monoclonal Laboratory for growing the monoclonal antibodies. This work was supported by the National Health and Medical Research Council of Australia (NHMRC) (637406), and the Victorian State Government Operational Infrastructure Support grant. A.Y. is a recipient of PhD scholarships from the Walter and Eliza Hall Institute of Medical Research as well as the University of Melbourne (Australia). A.F.C. is a Howard Hughes International Scholar. We thank Nicholas Lim for assistance with the SYBR Green-based invasion assays.

References

Aikawa, M., Miller, L.H., Johnson, J., and Rabbege, J. (1978) Erythrocyte entry by malarial parasites. A moving junction between erythrocyte and parasite. *J Cell Biol* **77:** 72–82.

Alexander, D.L., Mital, J., Ward, G.E., Bradley, P., and Boothroyd, J.C. (2005) Identification of the moving junction complex of *Toxoplasma gondii:* a collaboration between distinct secretory organelles. *PLoS Pathog* **1:** e17.

Allen, R.J., and Kirk, K. (2010) *Plasmodium falciparum* culture: the benefits of shaking. *Mol Biochem Parasitol* **169:** 63–65.

Andenmatten, N., Egarter, S., Jackson, A.J., Jullien, N., Herman, J.P., and Meissner, M. (2013) Conditional genome engineering in *Toxoplasma gondii* uncovers alternative invasion mechanisms. *Nat Methods* **10:** 125–127.

de Azevedo, M.F., Gilson, P.R., Gabriel, H.B., Simoes, R.F., Angrisano, F., Baum, J., *et al*. (2012) Systematic analysis of FKBP inducible degradation domain tagging strategies for the human malaria parasite *Plasmodium falciparum*. *PLoS ONE* **7:** e40981.

Bai, T., Becker, M., Gupta, A., Strike, P., Murphy, V.J., Anders, R.F., and Batchelor, A.H. (2005) Structure of AMA1 from *Plasmodium falciparum* reveals a clustering of polymorphisms that surround a conserved hydrophobic pocket. *Proc Natl Acad Sci USA* **102:** 12736–12741.

Bargieri, D., Lagal, V., Tardieux, I., and Menard, R. (2012) Host cell invasion by apicomplexans: what do we know? *Trends Parasitol* **28:** 131–135.

Bargieri, D.Y., Andenmatten, N., Lagal, V., Thiberge, S., Whitelaw, J.A., Tardieux, I., *et al*. (2013) Apical membrane antigen 1 mediates apicomplexan parasite attachment but is dispensable for host cell invasion. *Nat Commun* **4:** 2552.

Bell, A., Wernli, B., and Franklin, R.M. (1994) Roles of peptidyl-prolyl cis-trans isomerase and calcineurin in the mechanisms of antimalarial action of cyclosporin A, FK506, and rapamycin. *Biochem Pharmacol* **48:** 495–503.

Besteiro, S., Michelin, A., Poncet, J., Dubremetz, J.F., and Lebrun, M. (2009) Export of a *Toxoplasma gondii* rhoptry neck protein complex at the host cell membrane to form the moving junction during invasion. *PLoS Pathog* **5:** e1000309.

Boyle, M.J., Wilson, D.W., Richards, J.S., Riglar, D.T., Tetteh, K.K., Conway, D.J., *et al*. (2010) Isolation of viable *Plasmodium falciparum* merozoites to define erythrocyte invasion events and advance vaccine and drug development. *Proc Natl Acad Sci USA* **107:** 14378–14383.

Cao, J., Kaneko, O., Thongkukiatkul, A., Tachibana, M., Otsuki, H., Gao, Q., *et al*. (2009) Rhoptry neck protein RON2 forms a complex with microneme protein AMA1 in Plasmodium falciparum merozoites. *Parasitol Int* **58:** 29–35.

Chesne-Seck, M.L., Pizarro, J.C., Vulliez-Le Normand, B., Collins, C.R., Blackman, M.J., Faber, B.W., *et al*. (2005) Structural comparison of apical membrane antigen 1 orthologues and paralogues in apicomplexan parasites. *Mol Biochem Parasitol* **144:** 55–67.

Collins, C.R., Withers-Martinez, C., Hackett, F., and Blackman, M.J. (2009) An inhibitory antibody blocks interactions between components of the malarial invasion machinery. *PLoS Pathog* **5:** e1000273.

Collins, C.R., Das, S., Wong, E.H., Andenmatten, N., Stallmach, R., Hackett, F., *et al*. (2013) Robust inducible Cre recombinase activity in the human malaria parasite Plasmodium falciparum enables efficient gene deletion within a single asexual erythrocytic growth cycle. *Mol Microbiol* **88:** 687–701.

Cowman, A.F., and Crabb, B.S. (2006) Invasion of red blood cells by malaria parasites. *Cell* **124:** 755–766.

Crabb, B.S., Rug, M., Gilberger, T.W., Thompson, J.K., Triglia, T., Maier, A.G., and Cowman, A.F. (2004) Transfection of the human malaria parasite *Plasmodium falciparum*. *Methods Mol Biol* **270:** 263–276.

Crewther, P.E., Culvenor, J.G., Silva, A., Cooper, J.A., and Anders, R.F. (1990) *Plasmodium falciparum*: two antigens of similar size are located in different compartments of the rhoptry. *Exp Parasitol* **70:** 193–206.

Donahue, C.G., Carruthers, V.B., Gilk, S.D., and Ward, G.E. (2000) The *Toxoplasma* homolog of *Plasmodium* apical membrane antigen-1 (AMA-1) is a microneme protein secreted in response to elevated intracellular calcium levels. *Mol Biochem Parasitol* **111:** 15–30.

Drew, D.R., Hodder, A.N., Wilson, D.W., Foley, M., Mueller, I., Siba, P.M., *et al*. (2012) Defining the antigenic diversity of *Plasmodium falciparum* apical membrane antigen 1 and the requirements for a multi-allele vaccine against malaria. *PLoS ONE* **7:** e51023.

Gilson, P.R., and Crabb, B.S. (2009) Morphology and kinetics of the three distinct phases of red blood cell invasion by *Plasmodium falciparum* merozoites. *Int J Parasitol* **39:** 91–96.

Giovannini, D., Spath, S., Lacroix, C., Perazzi, A., Bargieri, D., Lagal, V., *et al*. (2011) Independent roles of apical membrane antigen 1 and rhoptry neck proteins during host cell invasion by apicomplexa. *Cell Host Microbe* **10:** 591–602.

Gonzalez, V., Combe, A., David, V., Malmquist, N.A., Delorme, V., Leroy, C., *et al*. (2009) Host cell entry by apicomplexa parasites requires actin polymerization in the host cell. *Cell Host Microbe* **5:** 259–272.

Gruring, C., Heiber, A., Kruse, F., Ungefehr, J., Gilberger, T.W., and Spielmann, T. (2011) Development and host cell

modifications of *Plasmodium falciparum* blood stages in four dimensions. *Nat Commun* **2:** 165.

Guerra, C.A., Howes, R.E., Patil, A.P., Gething, P.W., Van Boeckel, T.P., Temperley, W.H., *et al*. (2010) The international limits and population at risk of *Plasmodium vivax* transmission in 2009. *PLoS Negl Trop Dis* **4:** e774.

Harris, K.S., Casey, J.L., Coley, A.M., Masciantonio, R., Sabo, J.K., Keizer, D.W., *et al*. (2005) Binding hot spot for invasion inhibitory molecules on *Plasmodium falciparum* apical membrane antigen 1. *Infect Immun* **73:** 6981–6989.

Healer, J., Murphy, V., Masciantonio, R., Hodder, A.N., Gemmill, A.W., Anders, R., *et al*. (2004) Allelic polymorphisms in apical membrane antigen-1 are responsible for evasion of antibody-mediated inhibition in *Plasmodium falciparum*. *Mol Microbiol* **52:** 159–168.

Hehl, A.B., Lekutis, C., Grigg, M.E., Bradley, P.J., Dubremetz, J.F., Ortega-Barria, E., and Boothroyd, J.C. (2000) *Toxoplasma gondii* homologue of *Plasmodium* apical membrane antigen 1 is involved in invasion of host cells. *Infect Immun* **68:** 7078–7086.

Howell, S.A., Withers-Martinez, C., Kocken, C.H., Thomas, A.W., and Blackman, M.J. (2001) Proteolytic processing and primary structure of *Plasmodium falciparum* apical membrane antigen-1. *J Biol Chem* **276:** 31311–31320.

Janse, C.J., Franke-Fayard, B., Mair, G.R., Ramesar, J., Thiel, C., Engelmann, S., *et al*. (2006) High efficiency transfection of *Plasmodium berghei* facilitates novel selection procedures. *Mol Biochem Parasitol* **145:** 60–70.

Jullien, N., Sampieri, F., Enjalbert, A., and Herman, J.P. (2003) Regulation of Cre recombinase by ligand-induced complementation of inactive fragments. *Nucleic Acids Res* **31:** e131.

Lamarque, M., Besteiro, S., Papoin, J., Roques, M., Vulliez-Le Normand, B., Morlon-Guyot, J., *et al*. (2011) The RON2-AMA1 interaction is a critical step in moving junction-dependent invasion by apicomplexan parasites. *PLoS Pathog* **7:** e1001276.

Leykauf, K., Treeck, M., Gilson, P.R., Nebl, T., Braulke, T., Cowman, A.F., *et al*. (2010) Protein kinase a dependent phosphorylation of apical membrane antigen 1 plays an important role in erythrocyte invasion by the malaria parasite. *PLoS Pathog* **6:** e1000941.

Maier, A.G., Rug, M., O'Neill, M.T., Brown, M., Chakravorty, S., Szestak, T., *et al*. (2008) Exported proteins required for virulence and rigidity of Plasmodium falciparum-infected human erythrocytes. *Cell* **134:** 48–61.

Mital, J., Meissner, M., Soldati, D., and Ward, G.E. (2005) Conditional expression of *Toxoplasma gondii* apical membrane antigen-1 (TgAMA1) demonstrates that TgAMA1 plays a critical role in host cell invasion. *Mol Biol Cell* **16:** 4341–4349.

Mitchell, G.H., Thomas, A.W., Margos, G., Dluzewski, A.R., and Bannister, L.H. (2004) Apical membrane antigen 1, a major malaria vaccine candidate, mediates the close attachment of invasive merozoites to host red blood cells. *Infect Immun* **72:** 154–158.

Montero, E., Rodriguez, M., Oksov, Y., and Lobo, C.A. (2009) *Babesia divergens* apical membrane antigen 1 and its interaction with the human red blood cell. *Infect Immun* **77:** 4783–4793.

Narum, D.L., and Thomas, A.W. (1994) Differential localization of full-length and processed forms of PF83/AMA-1 an apical membrane antigen of *Plasmodium falciparum* merozoites. *Mol Biochem Parasitol* **67:** 59–68.

Poukchanski, A., Fritz, H.M., Tonkin, M.L., Treeck, M., Boulanger, M.J., and Boothroyd, J.C. (2013) *Toxoplasma gondii* sporozoites invade host cells using two novel paralogues of RON2 and AMA1. *PLoS ONE* **8:** e70637.

Richard, D., MacRaild, C.A., Riglar, D.T., Chan, J.A., Foley, M., Baum, J., *et al*. (2010) Interaction between *Plasmodium falciparum* apical membrane antigen 1 and the rhoptry neck protein complex defines a key step in the erythrocyte invasion process of malaria parasites. *J Biol Chem* **285:** 14815–14822.

Riglar, D.T., Richard, D., Wilson, D.W., Boyle, M.J., Dekiwadia, C., Turnbull, L., *et al*. (2011) Super-resolution dissection of coordinated events during malaria parasite invasion of the human erythrocyte. *Cell Host Microbe* **9:** 9–20.

Sambrook, J., Fritsch, E.F., and Maniatis, T. (1989) *Molecular Cloning: A Laboratory Manual*. Cold Spring Harbor, NY: Cold Spring Harbor Laboratory Press, pp. 12.14–12.29.

Singh, S., Alam, M.M., Pal-Bhowmick, I., Brzostowski, J.A., and Chitnis, C.E. (2010) Distinct external signals trigger sequential release of apical organelles during erythrocyte invasion by malaria parasites. *PLoS Pathog* **6:** e1000746.

Snow, R.W., Guerra, C.A., Noor, A.M., Myint, H.Y., and Hay, S.I. (2005) The global distribution of clinical episodes of *Plasmodium falciparum* malaria. *Nature* **434:** 214–217.

Srinivasan, P., Beatty, W.L., Diouf, A., Herrera, R., Ambroggio, X., Moch, J.K., *et al*. (2011a) Binding of Plasmodium merozoite proteins RON2 and AMA1 triggers commitment to invasion. *Proc Natl Acad Sci USA* **108:** 13275–13280.

Srinivasan, P., Beatty, W.L., Diouf, A., Herrera, R., Ambroggio, X., Moch, J.K., *et al*. (2011b) Binding of *Plasmodium* merozoite proteins RON2 and AMA1 triggers commitment to invasion. *Proc Natl Acad Sci USA* **108:** 13275–13280.

Suss-Toby, E., Zimmerberg, J., and Ward, G.E. (1996) Toxoplasma invasion: the parasitophorous vacuole is formed from host cell plasma membrane and pinches off via a fission pore. *Proc Natl Acad Sci USA* **93:** 8413–8418.

Thera, M.A., Doumbo, O.K., Coulibaly, D., Laurens, M.B., Ouattara, A., Kone, A.K., *et al*. (2011) A field trial to assess a blood-stage malaria vaccine. *N Engl J Med* **365:** 1004–1013.

Tiffert, T., Lew, V.L., Ginsburg, H., Krugliak, M., Croisille, L., and Mohandas, N. (2005) The hydration state of human red blood cells and their susceptibility to invasion by *Plasmodium falciparum*. *Blood* **105:** 4853–4860.

Tonkin, M.L., Roques, M., Lamarque, M.H., Pugniere, M., Douguet, D., Crawford, J., *et al*. (2011) Host cell invasion by apicomplexan parasites: insights from the co-structure of AMA1 with a RON2 peptide. *Science* **333:** 463–467.

Triglia, T., Healer, J., Caruana, S.R., Hodder, A.N., Anders, R.F., Crabb, B.S., and Cowman, A.F. (2000) Apical membrane antigen 1 plays a central role in erythrocyte invasion by *Plasmodium* species. *Mol Microbiol* **38:** 706–718.

Tyler, J.S., and Boothroyd, J.C. (2011) The C-terminus of *Toxoplasma* RON2 provides the crucial link between AMA1 and the host-associated invasion. complex. *PLoS Pathog* **7:** e1001282.

Vulliez-Le Normand, B., Tonkin, M.L., Lamarque, M.H., Langer, S., Hoos, S., Roques, M., *et al*. (2012) Structural and functional insights into the malaria parasite moving junction complex. *PLoS Pathog* **8:** e1002755.

Wilson, D.W., Crabb, B.S., and Beeson, J.G. (2010) Development of fluorescent *Plasmodium falciparum* for *in vitro* growth inhibition assays. *Malaria J* **9:** 152.

Wittayacom, K., Uthaipibull, C., Kumpornsin, K., Tinikul, R., Kochakarn, T., Songprakhon, P., and Chookajorn, T. (2010) A nuclear targeting system in *Plasmodium falciparum*. *Malaria J* **9:** 126.

Supporting information

Additional Supporting Information may be found in the online version of this article at the publisher's web-site:

Fig. S1. Southern blot analysis of W2mef/AMA1-loxP parasite clones. Of the eight clones isolated, seven has two tandem pAMA1-loxP plasmids integrated into the *Pfama1* gene locus resulting in two copies of the 3D7 *Pfama1* gene inserted. Clone #3 was selected for subsequent transfection of pDiCre.

Fig. S2. Identifying optimal rapamycin concentration for efficient DiCre activation with no off-target toxicity effects.

A. Rapamycin dose response curve was fitted using W2mef parasites. Rapamycin was added at ring-stage and incubated over one or two cycles of parasite replication. Parasite growth was determined by FACS and normalized against untreated W2mef parasites. IC50 of rapamycin was determined to be 2.7 μM, close to previously published results ($n = 2$; triplicate experiments) (Bell *et al*., 1994). Error bars indicate SD.

B. W2mef parasites incubated with varying amounts of rapamycin indicate that wild type parasite growth is not affected up to 300 nM of rapamycin. Beyond that, there is a dose dependent inhibition of growth. DMSO is inhibitory above 0.1% v/v ($n = 3$; triplicate experiments). Error bars represent SD.

C. Similar growth assays were performed on W2mef/AMA1-loxP parasites to confirm that at 300 nM or below, rapamycin does not induce observable growth inhibitory effect in the absence of DiCre expression.

Fig. S3. DiCre-mediated PfAMA1 knockdown has no adverse effects on intraerythrocytic development but lead to invasion inhibition.

A. Synchronized W2mef/AMA1-loxP/DiCre parasites were incubated with either 0.1% DMSO v/v or 0.1 μM rapamycin at early-to-mid ring stage. At 10, 20 and 35 h after the addition of rapamycin or DMSO, Giemsa smears were made. Parasitemia was measured and the proportion of ring, trophozoite or schizont stages is presented as a fraction of a pie chart. At all time points, the proportion of ring, trophozoite and schizont stages is comparable between the two treatments.

B. Closer inspection of parasite growth and reinvasion using SYBR Green I. DMSO-treated parasites displayed normal growth phenotype as the majority of the ring-stage parasites on day 0 progressed to late-stage parasites on day 1. On day 2, a majority of the late-stage parasites reinvaded to form new ring-stage parasites resulting in a doubling of total parasitemia. Total parasitemia may be higher if samples were processed later as not all of the late-stages have egressed and reinvaded. Parasites were split roughly 1:2 (between days 2 and 3) and 1:3 (between days 4 and 5) as denoted by the vertical dashed lines. A representative sample of a triplicate experiment is shown.

C. Rapamycin-treated parasites displayed normal intraerythrocytic growth but failed to invade normally. As expected, most of the ringstage parasites on day 0 progressed to late-stages on day 1 thereby confirming that rapamycin does not adversely affect parasite growth. Between days 1 and 2, however, total parasitemia had expanded from 2.7% to 3.7%, reflecting a 37% drop in invasion efficiency compared with DMSO-treated parasites. Invasion efficiency of rapamycin-treated parasites in comparison to DMSO-treated parasites varies in subsequent reinvasion cycles with a drop of 46% between days 3 and 4 and 18% between days 5 and 6. Parasites were split roughly 1:2 (between days 2 and 3) and 1:3 (between days 4 and 5) to be consistent with DMSO-treatment. A representative sample of a triplicate experiment is shown.

D. Representative flow cytometry plots showing different cell populations of ring-stage parasites, late-stage parasites and uninfected erythrocytes. Each column corresponds to a representative sample that was processed and stained with SYBR Green I about 24 h apart from the adjacent time point.

Table S1. List of primers used in this study.